THE DOE WATER CYCLE PILOT STUDY

BY N. L. MILLER, A. W. KING, M. A. MILLER, E. P. SPRINGER, M. L. WESELY, K. E. BASHFORD, M. E. CONRAD, K. COSTIGAN, P. N. FOSTER, H. K. GIBBS, J. JIN, J. KLAZURA, B. M. LESHT, M. V. MACHAVARAM, F. PAN, J. SONG, D. TROYAN, AND R. A. WASHINGTON-ALLEN

By pooling many sources of hydrologic information, a multilaboratory investigation of a watershed in Kansas identified ways to achieve closure of the water budget in observations and modeling.

In 1999, the U.S. Global Change Research Program (USGCRP) formed a Water Cycle Study Group (Hornberger et al. 2001) to organize research efforts in regional hydrologic variability, the extent to which this variability is caused by human activity, and the influence of ecosystems. The USGCRP Water Cycle Study Group was followed by a U.S. Department of Energy (DOE) Water Cycle Research Plan (Department of Energy 2002) that outlined an approach toward improving seasonal-to-interannual hydroclimate predictability and closing a regional water budget. The DOE Water Cycle Research Plan identified key research areas, including a comprehensive long-term observational database to support model development, and to develop a better understanding of the relationship between the components of local water budgets and large-scale processes. In response to this plan, a multilaboratory DOE Water Cycle Pilot Study (WCPS) demonstration project began with a focus on studying the water budget and its variability at multiple spatial scales.

Previous studies have highlighted the need for continued efforts to observationally close a local water budget, develop a numerical model closure scheme, and further quantify the scales in which predictive accuracy are optimal. A concerted effort within the National Oceanic and Atmospheric Administration (NOAA)-funded Global Energy and Water Cycle Experiment (GEWEX) Continental-scale International Project (GCIP) put forth a strategy to understand various hydrometeorological processes and phenomena with an aim toward closing the water and energy budgets of regional watersheds (Lawford 1999, 2001). The GCIP focus on such regional budgets includes the measurement of all components and reduction of the error in the budgets to near zero. To approach this goal, quantification of the uncertainties in both measure-

AFFILIATIONS: MILLER, BASHFORD, CONRAD, FOSTER, JIN, AND MACHAVARAM—Lawrence Berkeley National Laboratory, Berkeley, California; KING, GIBBS, PAN, AND WASHINGTON-ALLEN—Oak Ridge National Laboratory, Oak Ridge, Tennessee; MILLER AND TROYAN—Brookhaven National Laboratory, Upton, New York; SPRINGER AND COSTIGAN—Los Alamos National Laboratory, Los Alamos, New Mexico; WESELY, KLAZURA, AND LESHT—Argonne National Laboratory, Argonne, Illinois; SONG—Argonne National Laboratory, Argonne, and ANL Research Affiliate and Northern Illinois University, DeKalb, Illinois
CORRESPONDING AUTHOR: Norman L. Miller, 90-1116 One Cyclotron Road, Earth Sciences Division, Lawrence Berkeley National Laboratory, Berkeley, CA 94702
E-mail: nlmiller@lbl.gov
DOI:10.1175/BAMS-86-3-359

In final form 30 June 2004

ments and modeling is required. Model uncertainties within regional climate models continue to be evaluated within the Program to Intercompare Regional Climate Simulations (Takle et al. 1999), and model uncertainties within land surface models are being evaluated within the Program to Intercompare Land Surface Schemes (e.g., Henderson-Sellers 1993; Wood et al. 1998; Lohmann et al. 1998).

In the context of understanding the water budget at watershed scales, the following two research questions that highlight DOE's unique water isotope analysis and high-performance modeling capabilities were posed as the foci of this pilot study:

1) Can the predictability of the regional water budget be improved using high-resolution model simulations that are constrained and validated with new hydrospheric water measurements?
2) Can water isotopic tracers be used to segregate different pathways through the water cycle and predict a change in regional climate patterns?

To address these questions, numerical studies using regional atmospheric–land surface models and multiscale land surface hydrologic models were generated and, to the extent possible, the results were evaluated with observations. While the number of potential processes that may be important in the local water budget is large, several key processes were examined in detail. Most importantly, a concerted effort was made to understand water cycle processes and feedbacks at the land surface–atmosphere interface at spatial scales ranging from 30 m to hundreds of kilometers.

A simple expression for the land surface water budget at the watershed scale is expressed as

$$\Delta S = P + G_{\text{in}} - \text{ET} - Q - G_{\text{out}}, \tag{1}$$

where ΔS is the change in water storage, P is precipitation, ET is evapotranspiration, Q is streamflow, G_{in} is groundwater entering the watershed, and G_{out} is groundwater leaving the watershed, per unit time.

The WCPS project identified data gaps and necessary model improvements that will lead to a more accurate representation of the terms in Eq. (1). Table 1 summarizes the components of this water cycle pilot study and the respective participants. The following section provides a description of the surface observa-

Table 1. The set of WCPS tasks, what was done, and who did what is provided.

Tasks	What	Who
Data analysis	Jun–Jul–Aug (JJA) and Dec–Jan–Feb (DJF) storm events	
Archived climate data	WRW streamflow and precipitation, radar-based microphysics	Brookhaven National Laboratory (BNL)
	WRW baseline analysis	Argonne National Laboratory (ANL)
Archived isotope data	Obtain available water isotope rain gauge, stream gauge, flux data	Lawrence Berkeley National Laboratory (LBNL)
Archived surface data	Weather variables, LAI	Oak Ridge National Laboratory (ORNL), ANL
Modeling		
Atmospheric	48, 12, and 4 km resolution add water isotope mass conservation equations	LBNL
	48, 12, 4, and 1-km resolution	Los Alamos National Laboratory (LANL)
Land surface	Water, energy, momentum fluxes	All
Hydrology	Parameterized sub grid 1 km resolution	ANL
	Spatially distributed 30-m resolution with (δ^{18}O,δD) and validation	LBNL
Isotopes		
Isotope sampling	3–6 precip, 1 streamflow, 3 flux, soil water	LBNL, ANL
Isotope analysis	Analysis of δ^{18}O,δD	LBNL
Validation	Model and observation comparison	All

tion and modeling sites. This is followed by a section on model analyses, and then the summary and concluding remarks.

SITE DESCRIPTION. The Walnut River watershed (WRW), located in south-central Kansas, is about 6000 km^2, which is an order of magnitude smaller than the Atmospheric Radiation Measurement (ARM) Cloud Atmospheric Radiation Testbed (CART) site within which it is contained (Fig. 1). The major streams in the WRW are the Walnut River and its tributary, the Whitewater River. The two major reservoirs on the river system are El Dorado Lake and Winfield Lake. Surface water represents 91% of the water used in the WRW. Over 77% of the water use in WRW is for municipal purposes, with 10% for irrigation, 6.4% recreational use, and 3.3% industrial use (Kansas Water Office 1997).

This watershed is a partially closed basin (Karst geology prevents full closure) that is amenable to computing the components of the hydrological budget, and is sufficiently small to allow for reasonable observational coverage while having heterogeneous land cover types. The 1050 km^2 Whitewater watershed (WW) is located in the northwest portion of the WRW, and within the WW is the 12 km^2 Rock Creek (RC) watershed. These subdomains were selected for detailed observation and scaling studies partly because there are ongoing and previous studies here providing data and related information (LeMone et al. 2000).

The WRW has strong east–west terrain, precipitation, vegetation, and geological gradients. The surface elevation drops from about 500 m in the east to about 330 m in the southwest. Average precipitation in the eastern region is 86 cm yr^{-1}, and in the western region is 76 cm yr^{-1}. Approximately 65% of the precipitation falls between April and September, with an annual average snowfall of about 35-cm snow-water equivalent. The Walnut River floods once a year, on average, downstream of the town of Towanda (Fig. 1). Land use in the WW is approximately 65% cropland and 32% grassland, with the eastern region grassland, and the western region primarily cropland with urban expansion from nearby Wichita.

DATA MEASUREMENTS AND SAMPLING. Participants in the WCPS compiled an extensive database from archives (meteorology, vegetation types, topographic maps) and data obtained from a 1 April to 30 June 2002 intensive observation period (IOP). In addition, the WCPS conducted event and seasonal sampling and periodic vegetation mapping. Models were evaluated at three nested domains—the ARM CART, the WRW, and the WW (Fig. 1). In the subsections that follow, observations of components of the water budget in all three domains are presented. The observations consist of satellite retrievals of the leaf area index (LAI), which is a critical parameter in the evapotranspiration term in Eq. (1); measurements from local wells, which help constrain the groundwater terms in Eq. (1); and water isotopic tracers, which segregate water samples by physical processes.

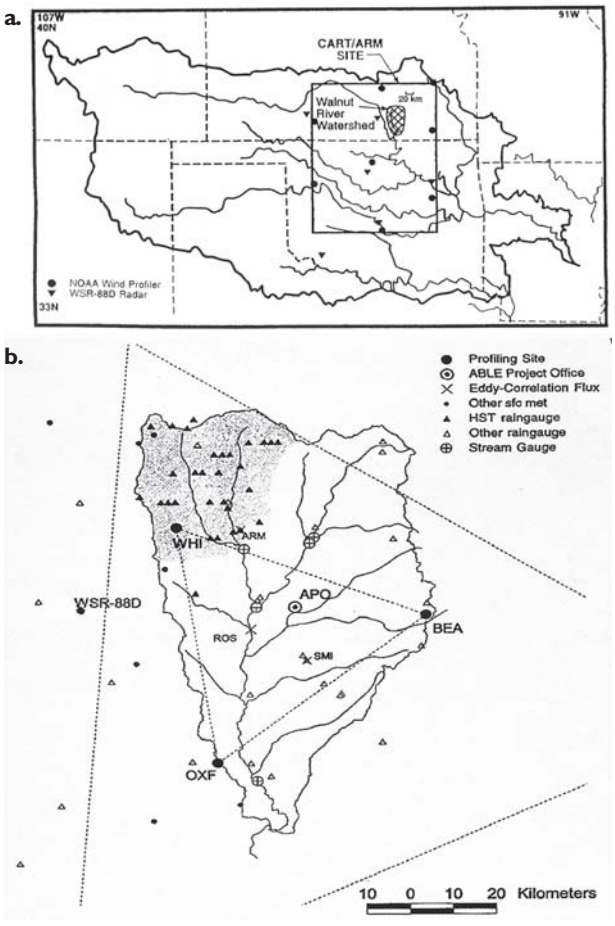

FIG. 1. (a) The ARM CART Southern Great Plains site, and (b) the Walnut River watershed with existing measurements.

Leaf area index measurements. Latent heat flux and surface albedo are sensitive to vegetation distribution, where the former is modulated by the valvelike action of the leaf stomata and the latter by the scattering characteristics of the leaf chlorophyll and leaf chemical composition. Both are intrinsically tied to the LAI, and should be represented accurately in water cycle models. In this study, spatially extensive ground-based measurements were collected on 111 plots (row crops, woodland, grassland, and pasture) across the entire WW in July 2002. The plots were 900 m^2 for comparison with the Landsat Enhanced Thematic Mapper

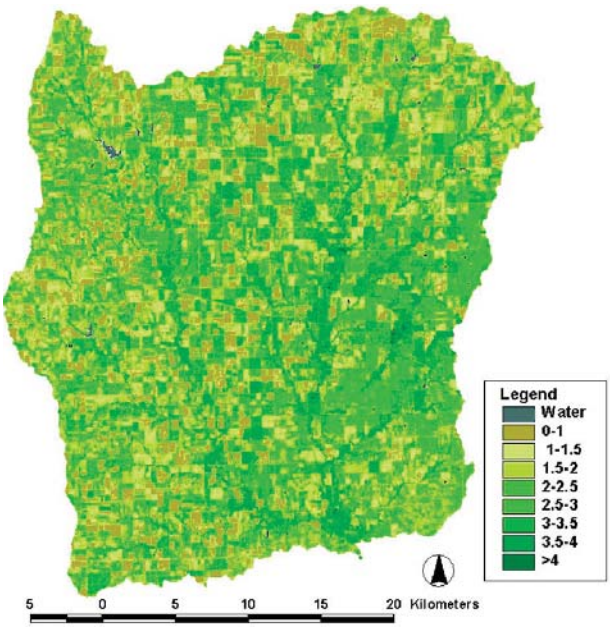

Fig. 2. Spatial distribution of LAI in the Whitewater watershed, simulated by applying empirical LAI–NDVI relationships to 30-m Landsat TM NDVI data collected in Jul 2002.

(TM)/ETM+ [see http://edc.usgs.gov/products/satellite/landsat7.html for more information on the Enhanced Thematic Mapper Plus (ETM+)] 30-m resolution.

The spatial distribution of LAI was estimated from satellite data using empirical relationships between the measured LAI and the normalized difference vegetation index (NDVI) derived from above-canopy measurements of reflectance obtained with a field radiometer. LAI–NDVI relationships were first established for three of the four vegetation types (row crops, grassland, and pasture) and, for variations of these types, combined statistically fitting measured LAI values to the corresponding NDVI values. Lack of canopy access precluded field measurement of woodland reflectance. The LAI–NDVI relationships were then applied to NDVI derived from the Landsat TM/ETM+ data, producing high-resolution LAI maps for WW.

Measured LAI values varied greatly within each vegetation type, with LAI–NDVI regression (r^2) values ranging from 0.66 to 0.78 for each vegetation type and for all types combined. Figure 2 shows LAI predicted for July 2002 from the LAI–NDVI relationship combining measurements for all cropland, grassland, and pasture plots. The 30-m resolution of the Landsat ETM+ data describes the spatial heterogeneity of LAI in the WW, with the spatially explicit LAI values well within the statistical distributions of field observations (Table 2).

In July 2002, the LAI across the WW varied spatially within each vegetation type from nearly bare ground to full canopy (Table 2). Accordingly, based on the model results for minimum (10th percentile) and maximum (90th percentile) LAI, the within-vegetation spatial LAI variability may result in spatial latent heat flux variability within a vegetation type as high as 400 W m^{-2} at midday (Fig. 3). For comparison, this spatial variability in both LAI and latent heat flux is comparable to the seasonal variability that might be observed for a warm mesic deciduous/cropland system. This analysis reinforces the need for accurate characterizations of spatial LAI variability to accurately simulate the finescale spatial latent heat flux variability.

Groundwater well and soil moisture transect measurements. The location of groundwater affects the energy balance and the exchange of latent heat because deeper-rooted vegetation may have access to this water, and the long-term soil moisture memory is linked to the deeper zone (Maxwell and Miller 2005). In the absence of surface reservoirs, groundwater also flows at a much slower rate than the other water fluxes in the budget equation [Eq. (1)]. As such, groundwater exhibits hysteresis in the local water cycle. Groundwater measurements performed for the WCPS represent a cursory attempt to provide insight into the groundwater response for the study period.

The hourly water elevation change in three wells (Potwin, B295, A272) for May 2002–March 2003 are shown in Figs. 4a–4c. Water-level fluctuations in these wells are on the order of 0.3 m or less. An indication of the annual cycle in groundwater elevation can be seen in Figs. 4b and 4c, but longer time series are needed to quantify the relationship between the local climate and groundwater response. Most importantly, the three-dimensional groundwater flow characteristics across the various domains examined in this study are unknown due to cost-constrained undersampling. Without a comprehensive groundwater measurement program, specification of the groundwater terms in the water budget is virtually impossible.

One set of soil moisture measurements was made

Table 2. Within-vegetation-type spatial variability in predicted LAI for Whitewater watershed. The minimum is defined by the 10th percentile, and the maximum by the 90th percentile, of the distribution of LAI values within a vegetation type.

Vegetation	Mean	Minimum	Maximum
Grassland	2.08	0.43	3.73
Row crop	2.11	0.46	3.78
Woodland	2.17	0.60	3.77

during the week of 6–8 May 2002 on recently tilled milo and wheat fields. A grid with a spacing of 30 m was sampled at 0.3-m spacing and at approximately 10-cm depth to examine small-scale variability. On the RC site, transects on the north side of the channel were established for surface soil moisture measurements on successive days between 5 and 7 June 2002.

Statistical analysis reveals a general drying of the area over the 3 days of observation. The mean soil moisture values ($cm^3\ cm^{-3}$) were 0.54, 0.51, and 0.49 for 5, 6, and 7 June, respectively (Fig. 5). The standard deviation increases from 3.59 on 5 June to 4.00 on 6 June, and 5.20 on 7 June. Again, these data represent a limited snapshot of the surface soil moisture distribution in the Whitewater River basin, but provide some points of reference against which to check the results of the simulation models.

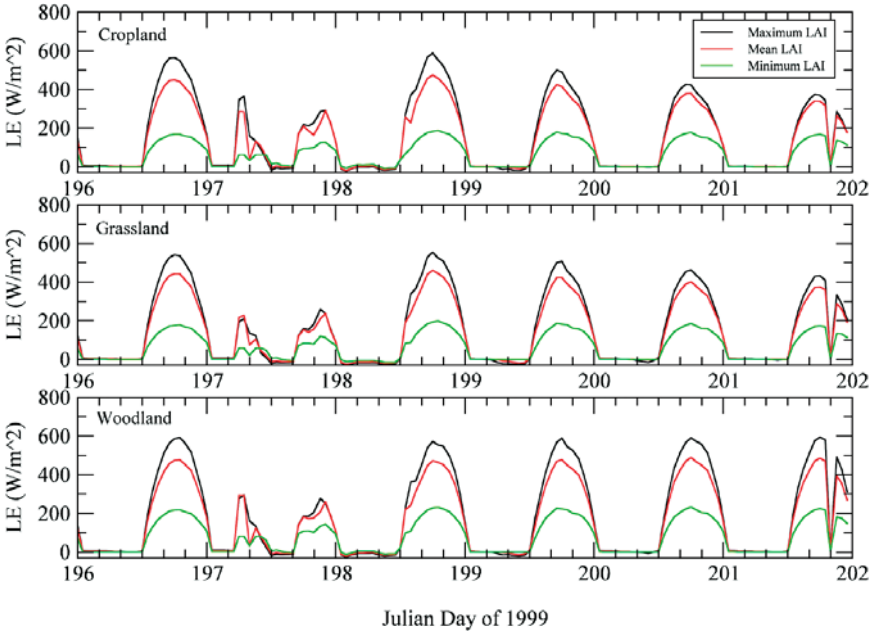

FIG. 3. TOPLATS-simulated latent heat flux for different vegetation types in the Whitewater watershed, assuming different values of LAI. See Table 2 for LAI values.

Water isotopic monitoring and sampling. The stable hydrogen and oxygen isotope ratios of atmospheric moisture vary depending on the source of the water, the extent of precipitation loss, and physical parameters (such as temperature and humidity). These relationships provide a critical link between local water cycle processes and the larger climate system. Isotope sampling helps to quantify terms in the water budget equation, while at the same time providing information on the historical movement of water that is currently a component of the local water cycle.

As part of the WCPS, an extensive study of the isotopic compositions of all components of the water cycle in the WRW was conducted. This work included event-based precipitation sampling (consisting of one or more samples of every significant storm) at two sites within the WRW. Samples of selected precipitation events were also collected from four other sites in the WRW to examine the spatial variability of precipitation at the watershed scale. To determine the isotopic composition of storm systems and related large-scale climate variations affecting the WRW, precipitation samples from 10 National Atmospheric Deposition Program (NADP) stations located along the primary storm tracks impacting the WRW were obtained. Additionally, water isotope samples of near-surface atmospheric vapor, surface water bodies, soil moisture, and groundwater were, and are still, collected every 3–4 months to monitor the response of isotopic compositions of components of the water cycle to seasonal and spatial variations in precipitation. During the IOP, a series of atmospheric vapor samples were collected at elevations up to 4000 m above the land surface to examine mixing between locally derived water vapor and moisture aloft. A detailed study of isotopic variations in the RC, a small tributary of the Whitewater River, in response to two intense storm events, was also undertaken to quantify the response of streamflow to specific precipitation events (Machavaram et al. 2003).

In general, the δD and $\delta^{18}O$ values of storm systems decrease with distance from the source (primarily the Gulf of Mexico, in this case), reflecting the progressive loss of higher δD and $\delta^{18}O$ precipitation. However, the isotopic compositions of precipitation are also affected by the addition of moisture from other sources, including evaporation of surface water and mixing with moisture from other storm tracks. The effect of secondary moisture from evapotranspiration can be estimated from changes in the deuterium excess of atmospheric vapor and precipitation. Initial isotopic measurements of the NADP and WRW rain samples show a systematic increase in the deuterium excess of precipitation as storms move from the Gulf of Mexico region northward into the WRW. Conversely, moisture derived

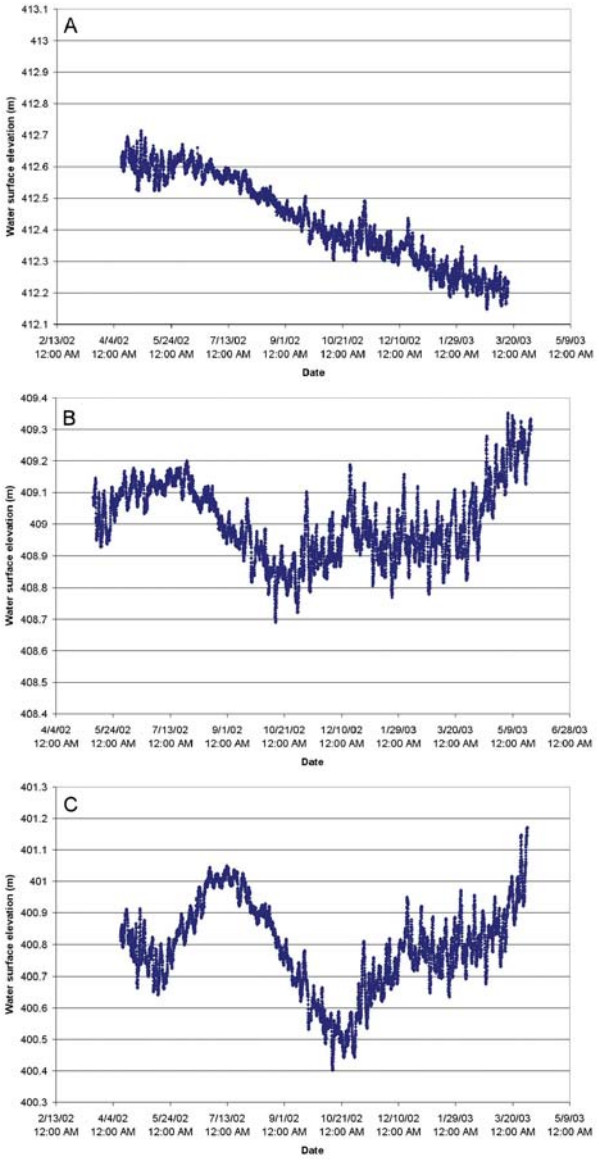

FIG. 4. Hourly water surface elevations for (a) well A272, a shallow saturated zone, (b) well B295, a deeper saturated zone, and (c) a Potwin supply well.

from the high-latitude jet stream causes significant drops in δD and $\delta^{18}O$ values of precipitation, especially during the colder winter months.

Figure 6a contains volume-weighted oxygen isotope ratios ($\delta^{18}O$) for precipitation samples collected from one site in the WRW. In general, the $\delta^{18}O$ values range from approximately –4‰ in the summer to –10‰ in the winter. However, the isotope data also vary in response to significant differences in the weather from one year to the next. In July–August 2001, mean temperatures were almost 3°C higher than during July–August 2002. Despite nearly identical rainfall totals, the average $\delta^{18}O$ and deuterium-excess values of the precipitation were significantly higher in 2001 (2.5‰ and 5‰, respectively), reflecting the increased role of moisture derived from the land surface during the warmer weather. Conversely, the mean temperature during October–November 2002 was 4°C lower than during October–November 2001, and there was unusually high precipitation during October 2002 (more than 3 times normal). The average $\delta^{18}O$ values of the precipitation samples collected during this period were approximately 1.5‰ lower than during October 2001, indicating a significant input of cold Arctic moisture derived from the high-latitude jet stream.

Both the general precipitation patterns and the extreme events also cause measurable shifts in the isotopic compositions of the rivers in the WRW (Fig. 6b). The $\delta^{18}O$ values of the Whitewater ranged between –4.4‰ and –5.9‰, with the summer samples greater than –5‰ and the winter samples less than –5.7‰, reflecting the general seasonal variations in precipitation. However, the two samples collected in the fall differed by 1.4‰ as a direct result of the intense, cold low-$\delta^{18}O$ storm system in October 2002. The $\delta^{18}O$ values of the Walnut River above its confluence with the Whitewater River were not strongly influenced by the precipitation because this section is primarily fed by water from the El Dorado Reservoir that has been shifted to higher $\delta^{18}O$ values due to evaporation. Because of the size of the reservoir, this water dominates flow in the Walnut River, causing its $\delta^{18}O$ values to remain relatively constant from –2.8‰ to –3.5‰. Downstream of the Whitewater River, the $\delta^{18}O$ value of the water is a mixture of the two signals, with the proportions varying due to the intensity of storm activity and the amount of water released from El Dorado Reservoir. For example, during October 2002 the $\delta^{18}O$ value of the lower Walnut River was closer to the $\delta^{18}O$ value of the Whitewater River due to the high precipitation levels during the fall of that year.

These data demonstrate the sensitivity of the isotope compositions of water to climatic factors impacting the water cycle. The regional precipitation data highlight the impacts of deviations from normal temperatures on the water cycle. Systematic changes in temperature due to factors such as global climate change should be readily recognizable. Monitoring the isotopic compositions of rivers and lakes provides a good, long-term average of precipitation patterns, modified by the effects of evaporation from the lakes (reservoirs) and infiltration of soil water. This also presents a potential monitor of the impacts of land-use changes (e.g., building reservoirs, increased crop irrigation, changes in vegetation) on the local water cycle. Ultimately, however, the most beneficial use of isotope

monitoring will be to validate numerical simulations of the water cycle in order to enable the use of these models for long-term predictions of the climate patterns.

MODELING AND ANALYSIS. Mesoscale models provide a medium for the comprehensive understanding of the processes that operate in the local water cycle, as well as a predictive capability. There have been a limited number of studies designed to evaluate the efficacy of the water cycle–related parameterizations used in mesoscale models, as well as tests of the sensitivity of the models to resolution (both vertical and horizontal). In this section, parameterizations in a coupled atmosphere–land surface model are compared to observations, and resolution sensitivity is tested. In addition to these analyses, code development on the implementation of stable water isotopes in a regional climate model is also discussed.

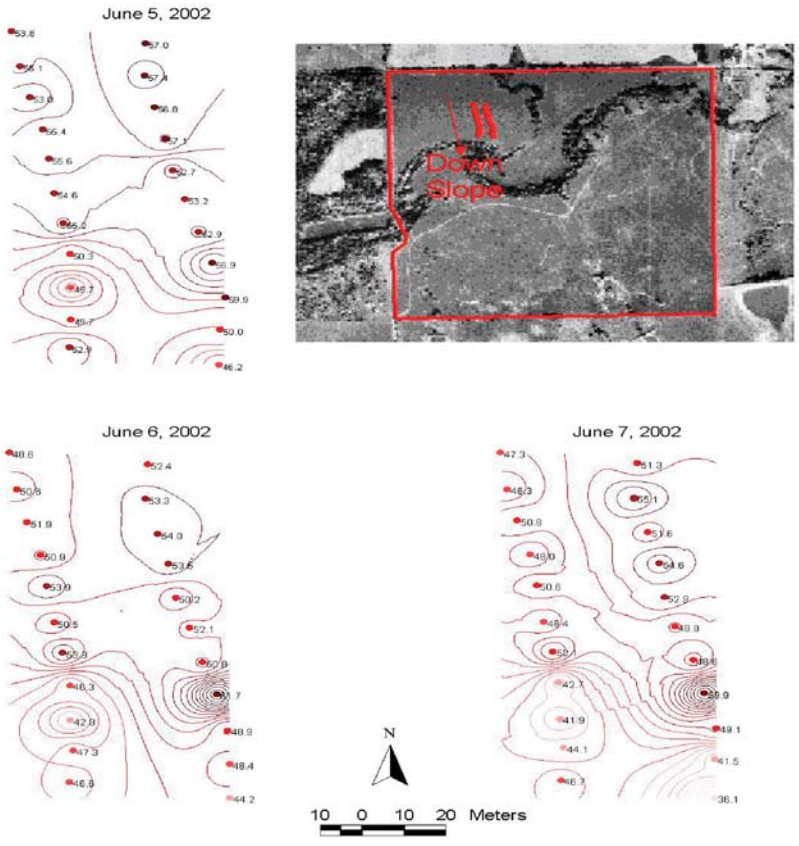

FIG. 5. Soil water contents from Rock Creek hillslope for the period 5–7 Jun 2002 measured with a portable time–domain reflectometry system.

Coupled mesoscale atmospheric–land surface modeling. The WCPS used two mesoscale atmospheric models—the fifth-generation Pennsylvania State University (PSU)–National Center for Atmospheric Research (NCAR) Mesoscale Model (MM5; Grell et al. 1995) and the Regional Atmospheric Modeling System (RAMS; Pielke et al. 1992). For both MM5 and RAMS, 48-km-resolution simulations of the continental United States and portions of the Pacific and Atlantic Oceans were generated. Nested 12-km-grid-resolution simulations focused on the High Plains, east of the Rocky Mountains to the eastern Midwest, and the 4-km-grid-resolution simulations were focused on the ARM CART domain.

AN EVALUATION OF MM5-SIMULATED AND WSR-88D-DERIVED PRECIPITATION. An evaluation of the precipitation simulated by MM5 using rain gauge–corrected rainfall estimates from the National Weather Service Weather Surveillance Radar-1988 Doppler (WSR-88D) was performed for the ARM CART domain and the WRW domain for March 2000 (Miller et al. 2003). Modeled and measured precipitation was compared to MM5

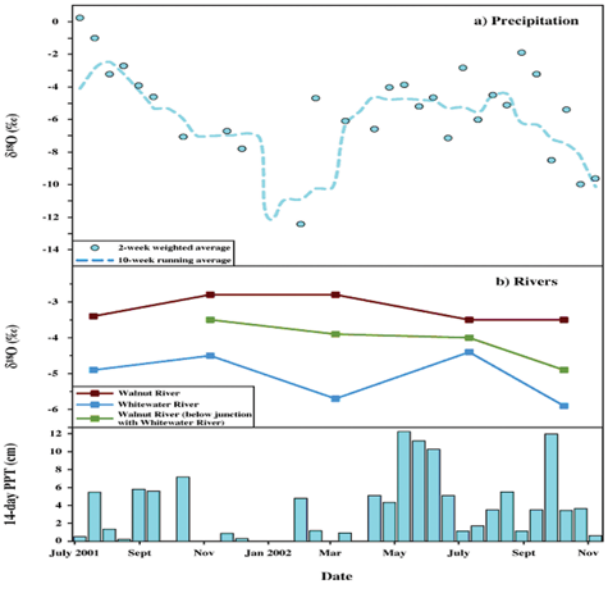

FIG. 6. (a) $\delta^{18}O$ concentration in precipitation at the APO. (b) $\delta^{18}O$ concentration in rivers at the Walnut River, Whitewater River, and at the junction of the Walnut and Whitewater Rivers. (c) Precipitation amounts at the ABLE Project Office (APO) site.

simulations at three resolutions (4, 12, and 48 km) to determine the impact of scale on the model's ability to predict precipitation.

The regional WSR-88D rain gauge–calibrated radar precipitation was provided by the National Weather Service's Arkansas–Red River Forecast Center. To evaluate the quality of the radar estimates, the rainfall measurements from March 2000 were compared to independent measurements collected using the high-resolution Atmospheric Boundary Layer Experiments (ABLE) rain gauge network in the WRW (11 gauges). Comparisons were made by matching the nearest ABLE rain gauge measurement with the nearest radar estimate in nonconvective conditions (Fig. 7). Two days were excluded from the analysis due to obvious convection. For the 27 days that were nonconvective, the total accumulated precipitation for the radar and rain gauge estimates was ~56 mm, and the two techniques differed in their measurements by 10 mm day^{-1} (Fig. 7). Hence, this point-to-point comparison suggests that the two techniques agree to within 20% in nonconvective situations. This result is somewhat expected in light of recent studies showing the vulnerability of radar-based precipitation estimates to the spatial variability of precipitation within the measurement volume (Miriovsky et al. 2004) and many past studies that demonstrate other susceptibilities, including precipitation phase and beam filling. It is assumed that the radar-based estimates for the entire ARM CART domain have similar differences.

MM5 was initialized and updated with the National Centers for Environmental Prediction (NCEP)–NCAR reanalysis II data, and the simulated cumulative 6-h precipitation was archived for March 2000 for the three different model resolutions. Radar-based rainfall estimates within each MM5 48- and 12-km grid cell were averaged to produce a rainfall estimate that could be directly compared with the MM5-simulated rainfall. The radar-based rainfall estimates had a typical resolution of 4–6 km over the ARM CART domain and approximately 5 km over the WRW domain, so no averaging was used for the 4-km comparison.

The MM5 6-h rainfall estimates over the WRW using 4-km resolution simulations, excluding the 2 days with obvious convection, show that MM5 underestimates precipitation by 60%, assuming that the radar estimates were accurate to within 20% (Fig. 8a). Although one event (day 3) seems to show a phase lag between the onset of precipitation in MM5 and observed precipitation, in general, the timing of precipitation events seems to be well represented by the model when it is run at 4-km resolution. The model has good skill at predicting the occurrence of precipitation, though it has less skill in predicting the amount of precipitation that was actually observed. Considering the entire ARM CART domain (Fig. 8b) improves overall agreement, but MM5 still underestimates precipitation by 37% for the month.

Similar comparisons for the 12- and 48-km simulations demonstrate that the agreement between modeled and measured precipitation is scale dependent for March 2000 (Table 3). As discussed above, the MM5 6-h forecast tends to underestimate the amount of precipitation that was actually observed at a 4-km resolution, regardless of the size of the domain used in the comparison. In contrast, the 12-km-resolution MM5 shows good skill at forecasting the total amount of

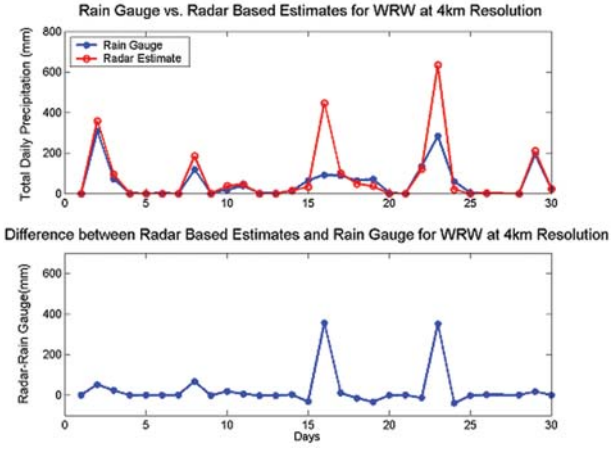

Fig. 7. Results from two independent rainfall estimates over the WRW using the Hydrologic Rainfall Analysis Data (HRAP) 4-km data.

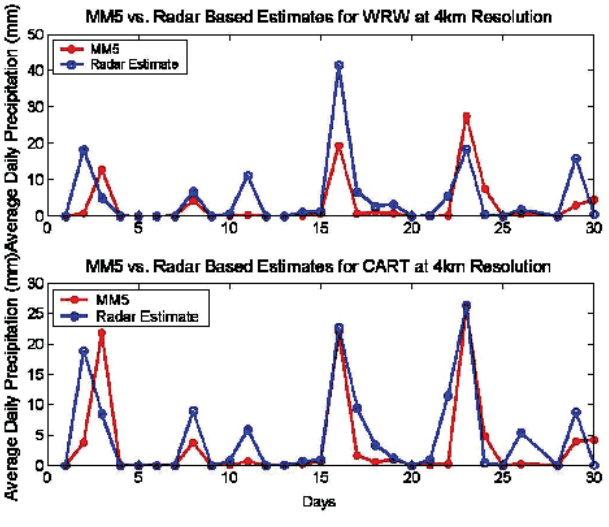

Fig. 8. MM5-simulated 4-km precipitation and WSR-88D-derived precipitation during Mar 2000 for (a) the WRW domain and (b) the ARM CART domain.

observed precipitation. At 48 km, the size of the comparison domain becomes an important issue; the precipitation in the WRW is significantly underestimated, while that over the ARM CART domain is well represented.

The variability in the radar-observed and MM5-simulated precipitation is also scale dependent. At 4 km, MM5 faithfully represents the observed variability in precipitation from point to point, while at 12-km resolution, the model, particularly in the WRW domain, overestimates variability in observed precipitation.

These results suggest that MM5 simulations of nonconvective rainfall over the WRW and the ARM Climate Research Facility (ACRF) site, which is approximately the size of a global climate model grid cell, are sensitive to the selected horizontal resolution, at least during the month that was analyzed here. This sensitivity should be analyzed in more detail in future studies and should be considered when using MM5 to simulate hydrologic processes—either as an independent entity, or as a future parameterization in a global climate model (Raisanen et al. 2004). It is difficult to make a credible attempt to evaluate the required accuracy of precipitation estimates, because it is both application dependent and integrally linked to other processes within the hydrologic system (i.e., evapotranspiration).

Table 3. Ratios of means (μ) and standard deviations (σ) between radar-measured and modeled precipitation over the WRW and the entire ARM CART site.

	μ (Radar)/ μ (MM5) [σ(Radar/ σ(MM5)]		
	4-km	12-km	48-km
WRW	1.68 [1.10]	1.07 [0.68]	1.32 [0.92]
CART	1.41 [1.14]	1.11 [0.84]	1.01 [0.83]

Implementation of water isotopes modeling in MM5. An important tool for testing the moisture process parameterizations in mesoscale models is to track stable water isotopes. Because the physical processes that alter isotopic ratios are well known, they can be used as benchmarks when simulated isotopic ratios are compared to observations. A stable isotope routine is being developed for MM5 (Foster et al. 2003). While a number of global climate models (GCMs) have isotope-tracing routines (Noone and Simmonds 2002; Jouzel et al. 1987), this will be one of the first regional climate models with such a scheme. A major obstacle to evaluating a regional isotope model is the lack of a dense network of isotopic measurements. The intensive observations and modeling carried out via the WCPS offers an opportunity to locally evaluate isotopic predictions of the regional climate model. As with the modeled rainfall versus radar, as well as the modeled vegetation cover versus satellite imagery, stable isotope simulations are being tested at several spatial scales. At the largest grid (48 km), the United States and parts of the Pacific and Atlantic Oceans are simulated. At this scale, tests for the observed trend of decreasing isotopic values along inland-heading transects, including from southern Texas to Oklahoma, used the data sampled from the NADP network. Because GCMs can capture similar latitudinal gradients (Jouzel et al. 1987), we expect the MM5/isotope model to be able to capture this signal. We will also examine the increase of the deuterium excess observed in Oklahoma relative to Texas. The nested grid with a 12-km resolution will be tested against the seasonal source signal in the isotopic values seen in Oklahoma. And, finally, we are attempting to use the nested 4-km-resolution simulations to reproduce the isotopic values of the atmospheric vapor samples collected over the WRW domain. Work has been initiated to reproduce the decreasing isotopic ratios observed in the 22–26 May 2002 convective events that were part of the IOP. Should these tests prove successful, we will be able to determine the sources of the local water, and to what extent it is advected into the region and locally reevaporated. The value of the deuterium excess has long been used as a proxy for the source of water, and this model will allow us to test this hypothesis on a small scale. This substudy is not yet complete, and forthcoming results will be reported elsewhere.

Finescale sensitivity simulations using RAMS. Another critical issue with the use of mesoscale models is the relationship between the models' vertical resolution and the amount and distribution of precipitation that it produces. Relatively fine vertical grid spacing can allow for better resolution of the vertical structure of the moisture and wind fields, but leads to higher computational costs. Simulations were generated with the four-nested-grid configuration of RAMS, employing two different vertical resolutions near the surface, and the precipitation results were compared as a test of the model's sensitivity to vertical resolution. The simulation with the finer vertical resolution used 50-m vertical grid spacing near the surface and a total of 46 vertical levels. At heights of 300 m above ground level (AGL), the grid spacing was gradually increased to 750 m. In the coarser vertical resolution case, the vertical grid spacing began at 200 m and increased above

400 m AGL to 750 m. In this run, 35 vertical levels were used. In both cases, the model top extended above 20 km.

Model predictions of the precipitation event on 2–3 March 2000 were compared between the two runs. Precipitation in the WRW began in the southern and western sections, with the Oxford precipitation gauge (Fig. 1) initially recording measurable amounts at about 1330 UTC on 2 March. The rain then spread to the east and north, ending in the WRW by roughly 1100 UTC on 3 March. RAMS predictions also indicate that the precipitation started in the southern and western sections of the watershed; however, both of the RAMS simulations tend to initiate the precipitation a couple of hours later than observed, and precipitation totals for the event were underpredicted, particularly at the two most northern rain gauge stations—Whitewater and Beaumont.

Comparing the two simulations with different vertical resolutions shows that precipitation totals were similar in the southern half of the watershed. In the RAMS simulation with the 50-m vertical grid spacing near the surface, the precipitation pattern moves to the east with little rain spreading to the northern sections of the watershed. The simulation with the 200-m vertical resolution produces a rainfall pattern that spreads to the east and north, and precipitation totals at the Whitewater and Beaumont locations are closer to, although still somewhat less than, that observed. Figure 9 presents the rainfall rates at 0000 UTC on 3 March 2000, as predicted by the two RAMS simulations. While the amounts are similar, the coarser vertical resolution places the greatest amounts further north, which leads to the greater precipitation predictions at the Whitewater and Beaumont sites.

Thus, for this single, nonconvective, synoptically driven case, finer vertical grid spacing near the surface does not dramatically affect precipitation totals estimated by the model. However, it does affect the horizontal distribution of the modeled precipitation within the WRW. In this case, the horizontal distribution is in better agreement with observations when the coarser vertical resolution is used. The results will likely be different for other cases, particularly where near-surface features, such as a low-level jet, play an important role; but, higher computational costs can be avoided by using coarser vertical resolution.

Land surface hydrologic modeling. The treatment of the land surface is an essential element of water cycle modeling. In this section, model results from two schemes are discussed.

SCALE ANALYSIS USING THE TOPMODEL-BASED LAND ATMOSPHERE TRANSFER SCHEME: TOPLATS. The land surface hydrologic model used here for evaluating scale dependent processes is the Topographic Model (TOPMODEL)-based Land–Atmosphere Transfer Scheme (TOPLATS; Famiglietti and Wood 1994). For this study, TOPLATS was set up and calibrated in several modes, including a fully distributed 30-m-resolution mode, a 30-m combined statistical–distributed mode (1-km probability distributions based on 30-m resolution data), a 1-km-resolution fully distributed mode, and a single-column mode. Several variations of these modes were calculated using uniform or distributed input forcing and characterizations. In the absence of finescale spatial observations, the 30-m-resolution fully distributed mode was used as a baseline for relative comparison of model performance. Simulations were from 1 January 1999 to 31 December 2000 for all modes, except the 30-m fully distributed mode, which was limited to 14 July–22 September 2000 due to computational demands. TOPLATS verification, based on comparison of the 1-km distributed model runoff data and the observed streamflow data at the Towanda gauge, had fair to good agreement, with a Nash efficiency of 0.65. TOPLATS modes were compared for the common 14 July–22 September 2000 time period.

Eleven simulations were performed with different modes, and with several varia-

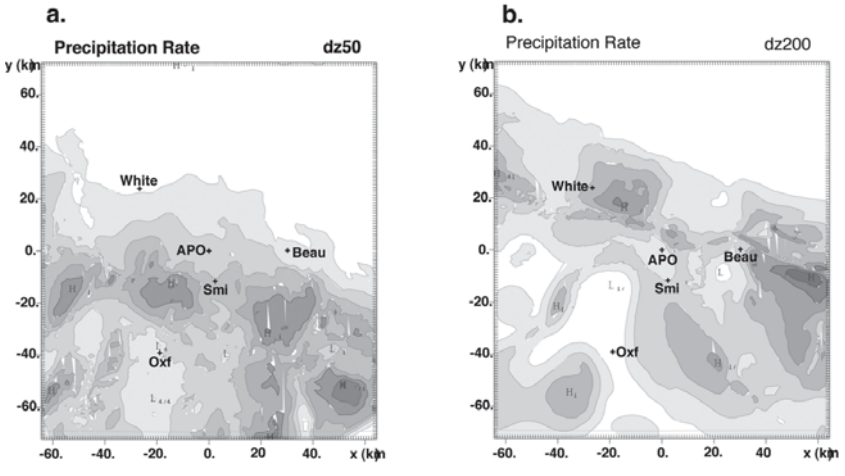

FIG. 9. The rainfall rates at 0000 UTC 3 Mar 2000, as predicted by the RAMS simulations with (a) 35 vertical levels and (b) 46 vertical levels.

tions in the representations of spatial variability of precipitation, land use, topography, and soils to assess the sensitivity of the model response (Table 4). Hourly precipitation was prescribed as uniform over the watershed, or at 1-km resolution. The land use and vegetation types were represented as uniform over the watershed at 1-km or 30-m resolutions, or 1-km distributions based on 30-m data. Using 30-m digital elevation model (DEM) data, topography index (the tangent of the ratio of the upstream flow area through a grid cell to the slope of the cell) distributions for the WW were determined. These represented the topography as uniform at 1-km resolution, and nonuniform at 1 km and 30 m for the whole catchment. Finally, the soil types were represented at 1-km resolution, or uniform over the watershed. For this study, TOPLATS was set up and calibrated in several modes, including a fully distributed 30-m resolution mode, a 30-m combined statistical-distributed mode, a 1-km-resolution fully distributed mode, and a single column mode (Bashford et al. 2002).

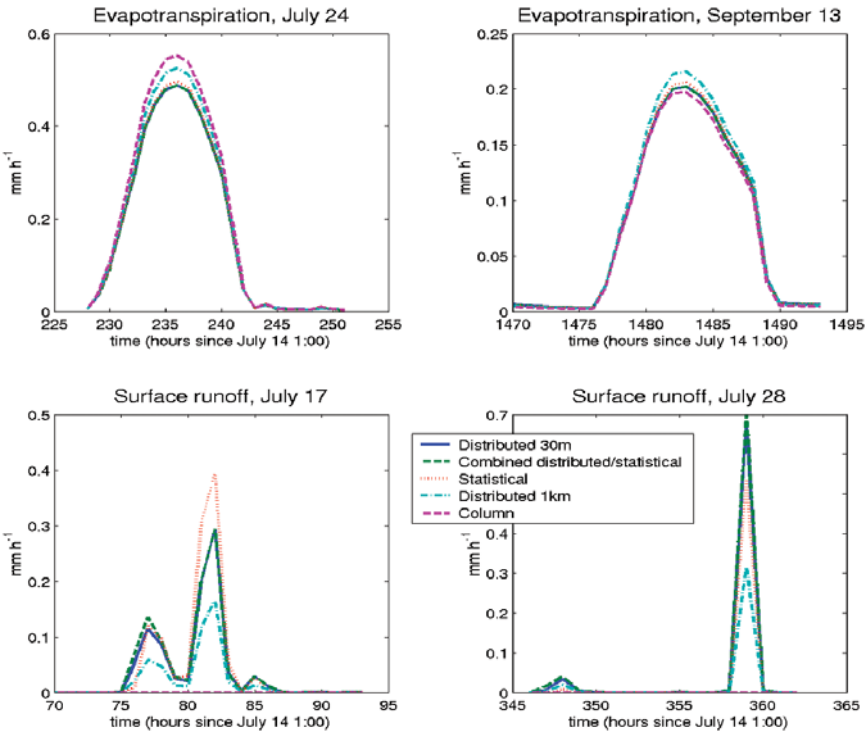

FIG. 10. Comparison of the 30-m distributed, combined statistical–distributed, 1-km distributed, and single column modes for (a) evapotranspiration on 24 Jul, (b) evapotranspiration on 13 Sep, (c) surface runoff for 17 Jul, and (d) surface runoff for 28 Jul 2000.

Model results suggest that in parts of the catchment evapotranspiration switched between being atmospherically controlled to soil-moisture controlled after 19 July. A comparison between the TOPLATS modes (Fig. 10) indicates that the combined distributed–statistical approach and the 30-m fully distributed mode (both evaluated at a 1-km resolution) resulted in near-identical water and energy fluxes, soil moisture, and runoff values. The statistical–distributed mode is significantly less computationally demanding and has far fewer parameters. The fully distributed 1-km resolution of TOPLATS led to an underestimate of runoff and an overestimate of evapotranspiration. The statistical mode resulted in an overestimate of runoff, and the column mode gave no runoff and had an extreme overestimate of evapotranspiration. Results of this study are summarized in Table 4a and 4b.

This study provides insight into how spatial variability can be represented without using a fully distributed model at finescale. The similarity between the spatially averaged data from the distributed–statistical and the fully distributed simulations suggests that the distributed–statistical mode is an effective way of reducing the computer resources required, while reproducing vertical fluxes. Lateral transport remains dependent on local information that is carried via a fully distributed mode.

PARAMETERIZATION OF SUBGRID-SCALE SURFACE MODEL. It is important for regional surface modeling to have accurate descriptions of subgrid and seasonal variations in surface fluxes, or biases may be introduced. To address this, and to aid in the study of the interannual variability of key surface hydrological components, the Parameterization of Subgrid-Scale Surface (PASS) model (Song et al. 2000a,b) focused on a 5-yr simulation (1996–2000) at the WRW. This study ties in with the TOPLATS study by providing finer-scale data with a longer simulation period. Long multiyear simulations and analyses with the fully distributed 30-m-resolution version of TOPLATS were not computationally feasible within the constraints of this pilot project.

The PASS model simulates land surface processes at subgrid scales up to 1 km and higher using a fairly simple approach to simulate evapotranspiration and

Table 4. Model experiment, description, and resolution. Rmse refers to root-mean-square error relative to the baseline case. (a) Resulting net flux, latent heat, sensible heat, and ground heat for each model experiment; (b) evapotranspiration, and surface and subsurface runoff; and (c) water table depth, and percent soil moisture (upper and lower) for each model experiment. Ws: uniform for watershed.

(a)	Net flux ($W\ m^{-2}$)		Latent ($W\ m^{-2}$)		Sensible ($W\ m^{-2}$)		Ground ($W\ m^{-2}$)	
BLFD30m	Mean	Rmse	Mean	Rmse	Mean	Rmse	Mean	Rmse
COMB	186.97	0.00	86.38	0.00	95.36	0.00	5.23	0.00
COMBpws	186.76	0.75	85.60	4.44	96.03	3.21	5.14	1.33
COMBtop1km	186.92	0.77	86.31	5.46	95.13	3.45	5.49	2.33
STAT	190.40	3.80	95.89	15.17	89.48	11.07	5.04	4.57
STATnotop	187.18	1.07	88.48	7.73	93.18	5.56	5.53	2.93
DIST1km	187.31	1.37	89.59	10.52	92.32	8.86	5.42	4.94
COL	190.17	3.46	93.90	13.00	91.22	8.70	5.06	3.68
	196.37	9.76	97.25	22.80	94.31	14.60	4.81	12.03

(b)	Evapotranspiration (mm)		Surface runoff (mm)		Subsurface runoff (mm)	
	Mean	Rmse	Mean	Rmse	Mean	Rmse
BLFD30m	0.128	000	9.232E–03	000	2.605E–04	000
COMB	0.127	6.548E–03	9.486E–03	2.040E–03	2.589E–04	1.990E–06
COMBpws	0.128	8.063E–03	9.764E–03	9.157E–03	2.582E–04	2.651E–06
COMBtop1km	0.142	2.255E–02	9.023E–03	1.724E–03	2.423E–04	1.865E–05
STAT	0.131	1.142E–02	1.087E–02	2.620E–02	2.300E–03	2.216E–03
STATnotop	0.133	1.559E–02	000	1.149E–01	3.593E–03	3.369E–03
DIST1km	0.140	1.934E–02	4.998E–03	5.396E–02	3.082E–04	5.244E–05
COL	0.145	3.386E–02	000	1.149E–01	3.402E–03	3.179E–03

(c)	Water table depth (mm)		Soil moisture Upper zone		Soil moisture Lower zone	
	Mean	Rmse	Mean	Rmse	Mean	Rmse
BLFD30m	1924	0.00	0.337	0.0000	0.336	0.0000
COMB	1924	0.77	0.337	0.0012	0.337	0.0011
COMBpws	1925	1.25	0.336	0.0025	0.336	0.0004
COMBtop1km	1947	25.86	0.340	0.0052	0.354	0.0186
STAT	1962	39.54	0.340	0.0046	0.342	0.0056
STATnotop	1818	123.49	0.316	0.0224	0.325	0.0208
DIST1km	1870	58.55	0.331	0.0065	0.340	0.0104
COL	1833	108.20	0.314	0.0250	0.315	0.0299

Effect of varying representation of spatial variability on water table depth and soil moisture (catchment average). (Rmse refers to root-mean-square error relative to the baseline case.)

Experiment	Description	Resolution
BLFD	Baseline (distributed)	30 m
COMB	Combined (distributed 1 km with 30-m index)	1 km/30 m
COMBpws	Combined, uniform precipitation	1 km/30 m
STAT	Statistical	30 m
STATnotop	Statistical	30 m
COL	Lumped column	ws

root zone–available soil moisture (RAM). It is based, in part, on Advanced Very High Resolution Radiometer (AVHRR)-derived NDVI data and conventional surface meteorological data. Biweekly composite 1-km-resolution NDVI values processed by the U.S. Geological Survey (USGS) were adjusted to compensate for atmospheric effects producing surface estimates of NDVI. The spatial NDVI variability is large and occurs on scales smaller than 1 km. Long-term simulation of evapotranspiration using PASS requires continuous biweekly data on surface conditions.

The 5-yr input dataset was constructed from meteorological observations at the WRW and the ARM CART extended facility near Towanda. WRW surface precipitation consisted of 4-km-resolution radar data that were adjusted with rain gauge observations sup-

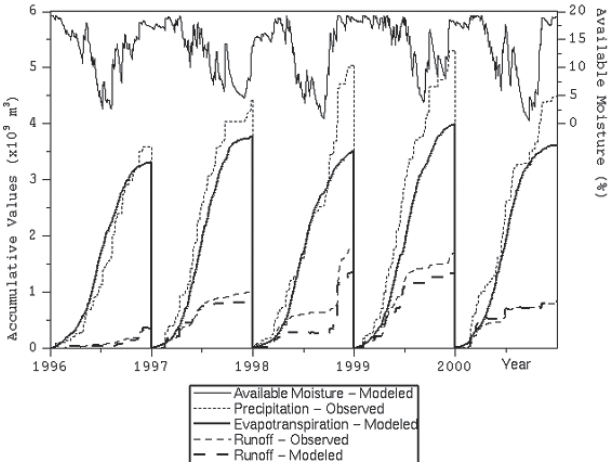

Fig. 11. Modeled and observed yearly accumulative values of surface hydrological components at the WRW and modeled root zone–available moisture during 1996–2000.

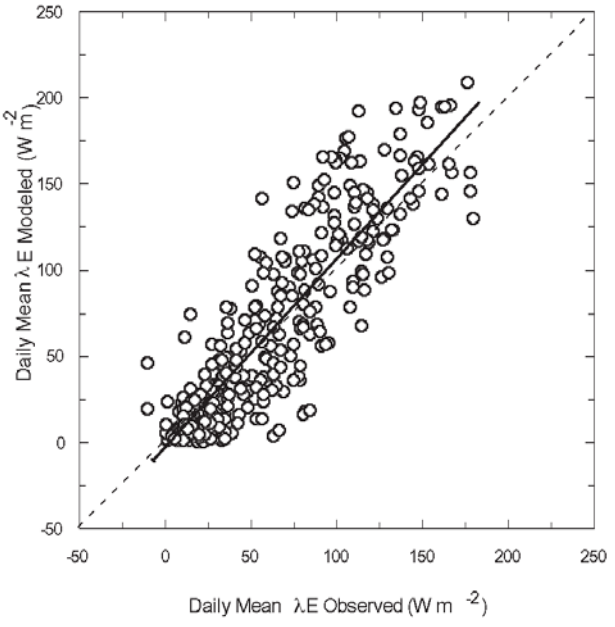

Fig. 12. Comparison of modeled versus observed daily mean latent heat fluxes in 2000 at the Whitewater site. The solid line represents a linear regression fit.

plied by the Arkansas–Red River Forecast Center. Daily streamflow data at Winfield (Fig. 2) were obtained from the USGS and compared to PASS runoff estimates, which were derived as the residual term in the water balance.

The initial RAM value for all pixels was assumed to be the maximum value, that is, the available moisture capacity for the dominant soil type in each pixel, and surface runoff was assumed to occur when the estimated RAM exceeded this value. This water excess was assumed to be lost from soil layers contributing to evapotranspiration, but the additions to local streamflow and groundwater recharge were not estimated in this simple model. Total runoff was assumed to be the difference between precipitation and evapotranspiration if the RAM for the entire WRW is the same at the end of the computational period as it was at the beginning, and if water losses through the bedrock were negligible. Also, the amount of time for the water balance computations should be sufficiently long to relegate changes in soil and groundwater storage to small contributions relative to precipitation and evaporation. Figure 11 shows the result for this method of runoff calculation, relative to the streamflow at the Winfield stream gauge station. The average RAM calculated for the WRW is lowest in the late summer, when rainfall is limited and evaporative demand is high, and is highest in the winter. Except for the transition between 1997 and 1998, this soil moisture storage appears to be consistently at very large values at the end of the yearly computational periods.

Over the 5-yr period, the modeled water loss from evapotranspiration at the end of each year accounts for 70%–90% of precipitation, which is reasonable for southern Kansas. The differences between the observed streamflow and modeled runoff are less than 25% and seem to depend on the precipitation amount and

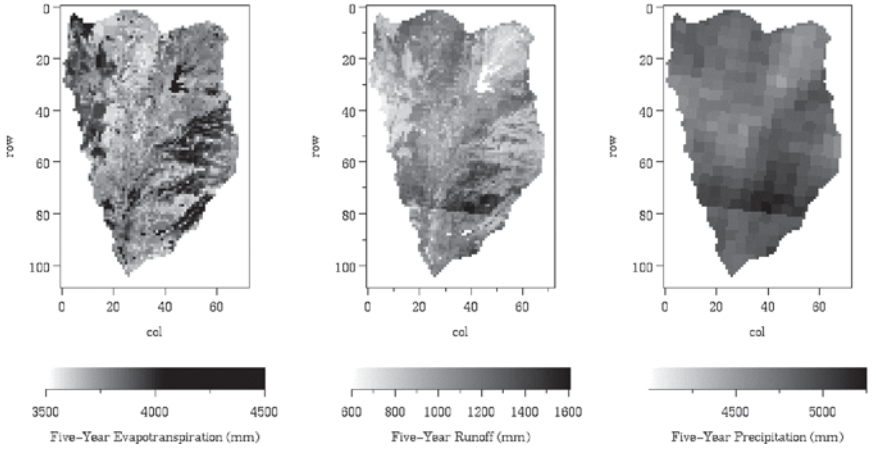

Fig. 13. (left) Total modeled evapotranspiration, (middle) total modeled runoff, and (right) observed precipitation for the WRW during 1996–2000.

distributions. For example, the differences are smaller for 1996 and 2000, when precipitation was spread evenly throughout the year, than for 1998 and 1999, when large precipitation events occurred rather late in the year. Relatively large evapotranspiration rates, beginning in the summer of 1997, led to the lower RAM at the end of the year, and the resulting deficit in the soil moisture in early 1998 led to reduced runoff until a large precipitation event occurred in October. Rather large evapotranspiration rates were also simulated for the summer of 1999, mostly driven by high precipitation rates that increased RAM. Overall, the modeled runoff is less than or equal to the observed streamflow, suggesting that modeled evapotranspiration estimates might be too large. It is suspected that when the rain rate is high, more runoff occurs as a result of a limited infiltration rate. This process will be considered in the next set of PASS model improvements.

To allow for examination of some of the details of evapotranspiration, modeled and observed daily means of latent heat fluxes at WW are plotted (Fig. 12). While the variations appear to be well captured, the best-fit line is slightly steeper than the 1:1 line, indicating some model overestimation. Large spatial variation exists even for the 5-yr total accumulated values (Fig. 13). The pattern of higher evapotranspiration corresponds to higher precipitation pixels, except in the southern part of the WRW, where an east–west belt of higher precipitation corresponds to higher runoff. Several strong precipitation events had occurred along this east–west belt in the southern WRW. On average, evaporative water loss accounts for nearly 80% of precipitation, and runoff accounts for 20%.

Preliminary results indicate that accumulative surface evapotranspiration was slightly overestimated, which resulted in underestimates of cumulative runoff within the WRW as compared to observed streamflow at the outlet of the WRW; the maximum yearly underestimate was 25% in 1998. Diurnal and seasonal changes in modeled evapotranspiration in 2000 matched fairly well with the in situ flux measurements despite a slight overestimation in cumulative evaporative water loss during certain periods at certain sites. These results suggest that a highly parameterized surface model is of value, but PASS can be improved to efficiently estimate long-term surface hydrological components. It is expected that continued work on the selection of proper root-zone depths for various types of vegetation and on runoff process treatment will improve the water budget.

SUMMARY AND RECOMMENDATIONS. The WCPS study represents an organized effort to pool many sources of hydrologic data to provide a framework for evaluating the hydrologic cycle via regional models and to better understand the requirements for linking such regional processes to climatic-scale forces that modulate the water cycle. It was centered on the use of observations and modeling toward closing the water budget of a small, representative watershed, and understanding the links between large- and local-scale processes that modulate the water budget.

Primary findings based on the two research questions addressing water budget closure are summarized below.

The latent heat flux shows large variability at small scales (< 1 km) and is sensitive to the spatial distribution of vegetation, soil moisture, access of deep-rooted plants to groundwater, and local atmospheric processes. While considerable information about the surface characteristics can be gained from satellite retrievals, sufficient in situ measurements to evaluate these retrievals and existing parameterizations (e.g., TOPLATS and PASS) are seriously lacking. Achieving true closure of the water budget of the WRW will require a long-term, coordinated measurement campaign to quantify components of the latent heat flux and measurement uncertainty.

Soil moisture and deeper groundwater measurements are scarce in the WRW. Soil moisture varies considerably on scales of only a few meters, and a detailed and coordinated measurement campaign would be required to properly quantify these variations. To achieve observational closure, it would be necessary to sample soil moisture regularly and with sufficient resolution to resolve the largest sources of variance (100 m or less). While satellite measurements may provide a gross measure of soil moisture, they do not have sufficient resolution to achieve the process-level understanding that is required to evaluate model representations. Deeper groundwater is expensive to measure and was grossly undersampled during the WCPS, mostly due to cost. Observational closure in the WRW would require a sampling strategy that is linked to the geological structure of the region and a coordinated measurement strategy.

There is a wealth of precipitation data available for the WRW. Notwithstanding, there remains considerable uncertainty in the radar-based measurement of precipitation, although polarized radar is known to provide better estimates. Simulations with MM5 and RAMS suggest that the precipitation parameterizations used in the models are sensitive to vertical and horizontal resolution. The WCPS suggests that a concerted effort to measure and model precipitation in the WRW would involve the long-term use of polarized radar, a dense network of independent rain gauges (gauges not used

in the radar-precipitation algorithm), and a comprehensive study of model performance over many seasons.

Observational closure of the water budget in the WRW would require systematic measurement of streamflow at all exit branches, rather than measurements designed primarily for flood forecasting. Reservoir levels would also have to be measured, along with the water levels in larger farm ponds.

Long-term monitoring of isotopic fractionations in the WRW would provide the necessary links to the climate system and a pathway for examining feedbacks within the system. Isotopic monitoring of runoff, precipitation, and groundwater, combined with model simulations of isotopic fractionations, would provide a medium for understanding shortfalls in the models and provide a key element in water cycle prediction by linking specific conditions within the watershed with the large-scale transport of water from its sources.

ACKNOWLEDGMENTS. This work was supported by the U.S. Department of Energy, Office of Science, Office of Biological and Environmental Research under contract DE-AC03-76F00098 for LBNL, contract DE-AC05-00OR22725 for ORNL, contract DE-AC02-98CH10886 for BNL, contract W-7405-ENG-36 for Los Alamos, and contract W-31-109-Eng-38 for ANL. Individuals who contributed to this study include Susan Kemball-Cook and Don DePaolo at LBNL, Tracy Schofield and Peter Beeson at LANL, David Cook, Donna Holdridge, Richard Coulter, and Timothy Martin at ANL, and Vonekia Atkinson, Selena Mellon, and Mike Sale at ORNL. This manuscript is LBNL Report LBNL-53826. *The DOE Water Cycle Pilot Study is dedicated to the memory of Dr. Marvin L. Wesely.*

REFERENCES

Bashford, K. E., H. O. Sharif, W. T. Crow, N. L. Miller, E. F. Wood, 2003: An investigation of scale and spatial variability using fully- and semi-distributed TOPLATS at the Whitewater Watershed, Kansas. *Extended Abstracts, 17th Conf. on Hydrology,* Long Beach, CA, Amer. Meteor. Soc., P1.12.

Department of Energy, 2002: The Water Cycle Research Strategy. Office of Biological and Environmental Research, DOE SC-0043.

Famiglietti, J. S., and E. F. Wood, 1994: Multi-scale modeling of spatially variable water and energy balance processes. *Water Resour. Res.,* **30,** 3061–3078.

Foster, P. N., N. L. Miller, and D. J. DePaolo, 2003: Implementation and testing of water isotopes into a regional climate model. *Abstracts, Workshop on Isotope Tracers in Water Cycle Models,* Sapporo, Japan, IAHS/ICT, IAEA, B.360.

Grell, G., J. Dudhia, and D. R. Stauffer, 1995: A description of the Fifth-Generation Penn State/NCAR Mesoscale Model (MM5). NCAR Tech. Note NCAR/TN-398+STR, 117 pp.

Henderson-Sellers, A., Z.-L. Yang, and R. E. Dickinson, 1993: The project for intercomparison of land surface schemes. *Bull. Amer. Meteor. Soc.,* **74,** 1335–1349.

Hornberger, G. M., J. D. Aber, J. Bahr, R. C. Bales, K. Beven, E. Foufoula-Georgiou, G. Katul, J. L. Kinter III, R. D. Koster, D. P. Lettenmaier, D. McKnight, K. Mitchell, J. O. Roads, B. R. Scanlon, and E. Smith. 2001: *A plan for A New Science Initiative On Global Water Cycle.* US Global Change Research Program, Washington, DC, 81 pp.

Jouzel, J., G. L. Russell, R. J. Suozzo, R. D. Koster, J. W. C. White, and W. S. Broecker, 1987: Simulations of the HDO and H218O atmospheric cycles using the NASA GISS general circulation model: The seasonal cycle for present-day conditions. *J. Geophys. Res.,* **92,** 14 739–14 760.

Kansas Water Office, cited 1997: Walnut Basin Advisory Committee. [Available online at www.kwo.org/Org_People/walnut.htm.]

Lawford, R. G., 1999: A midterm report on the GEWEX Continental-scale International Project (GCIP). *J. Geophys. Res.,* **104,** 19 279–19 292.

——, 2001: Integration of land observations and modeling: Experiences and strategies of a large scale experiment. *Land Surface Hydrology, Meteorology, and Climate: Observations and Modeling,* V. Lakshmi, J. Albertson, and J. Schaake, Eds., Vol. 3, *Water Science and Application,* Amer. Geophys. Union, 215–230.

LeMone, M. A., and Coauthors, 2000: Land–atmosphere interaction research, early results, and opportunities in the Walnut River Watershed in southeast Kansas: CASES and ABLE. *Bull. Amer. Meteor. Soc.,* **81,** 757–779.

Lohmann, D., and Coauthors, 1998: The Project for Intercomparison of Land Surface Schemes (PILPS): Phase 2C, Red-Arkansas River Basin experiment, 3, Spatial and temporal analysis of water fluxes. *Global Planet. Change,* **19,** 161–176.

Machavaram, M. V., M. E. Conrad, and N. L. Miller, 2003: Precipitation induced variations in streamflow. *Extended Abstracts, 17th Conf. on Hydrology,* Long Beach, CA, Amer. Meteor. Soc., JP3.12.

Maxwell, R. M., and N. L. Miller, 2005: On the development of a coupled land surface and groundwater model. *J. Hydrometeor.,* in press.

Miller, M. A., D. T. Troyan, N. L. Miller, J. Jin, S. Kemball-Cook, and K. R. Costigan, 2003: Water cycle variability over a small watershed: A one month

comparison of measured and modeled precipitation over the Southern Great Plains. *Extended Abstracts, Observing and Understanding the Variability of Water in Weather and Climate*, Long Beach, CA, Amer. Meteor. Soc., 4.8.

Miriovsky, B. J., and Coauthors, 2004: An experimental study of small-scale variability of radar reflectivity using disdrometer observations. *J. Appl. Meteor.,* **43,** 106–118.

Noone, D., and I. Simmonds, 2002: Associations between $\delta^{18}O$ of water and climate parameters in a simulation of atmospheric circulation for 1979–95. *J. Climate,* **15,** 3150–3169.

Pielke, R. A., and Coauthors, 1992: A comprehensive meteorological modeling system—RAMS. *Meteor. Atmos. Phys.,* **49,** 69–91.

Raisanen, P., H. W. Barker, M. F. Khairoutdinov, J. N. Lin, and D. A. Randall, 2004: Stochastic generation of subgrid-scale cloudy columns for large-scale columns. *Quart. J. Roy. Meteor. Soc.,* **130,** 2047–2067.

Song, J., M. L. Wesely, R. L. Coulter, and E. A. Brandes, 2000a: Estimating watershed evapotranspiration with PASS. Part I: Inferring root-zone moisture conditions using satellite data. *J. Hydrometeor.,* **1,** 447–461.

——, ——, M. A. LeMone, and R. L. Grossman, 2000b: Estimating watershed evapotranspiration with PASS. Part II: Moisture budget during drydown periods. *J. Hydrometeor.,* **1,** 462–473.

Takle, E. S., and Coauthors, 1999: Project to Intercompare Regional Climate Simulations (PIRCS): Description and initial results. *J. Geophys. Res.,* **104,** 19 443–19 461.

Wood, E. F., and Coauthors, 1998: The project for intercomparison of land-surface parameterization schemes (PILPS) phase 2(c) Red-Arkansas River basin experiment: 1. Experiment description and summary intercomparisons. *Global Planet. Change,* **19,** 115–135.